


Case Report

A case of recurrent epilepsy-associated rosette-forming glioneuronal tumor with anaplastic transformation in the absence of therapy

Aaron Halfpenny,¹  Sean P. Ferris,² Marjorie Grafe,¹ Randy Woltjer,¹ Nathan Selden,¹ Kellie Nazemi,¹ Arie Perry,² David A. Solomon,² Sakir H. Gultekin,^{1,3} Stephen Moore,¹ Susan Olson,¹ Helen Lawce,¹ Lora Lucas,¹ Christopher L. Corless¹ and Matthew D. Wood¹

¹Department of Pathology, Oregon Health & Science University, Portland, Oregon, ²Department of Pathology, University of California, San Francisco, San Francisco, California and ³Department of Pathology and Laboratory Medicine, University of Miami, Holtz Children's Hospital, Miami, Florida, USA

Rosette-forming glioneuronal tumor (RGNT) most commonly occurs adjacent to the fourth ventricle and therefore rarely presents with epilepsy. Recent reports describe RGNT occurrence in other anatomical locations with considerable morphologic and genetic overlap with the epilepsy-associated dysembryoplastic neuroepithelial tumor (DNET). Examples of RGNT or DNET with anaplastic change are rare, and typically occur in the setting of radiation treatment. We present the case of a 5-year-old girl with seizures, who underwent near total resection of a cystic temporal lobe lesion. Pathology showed morphologic and immunohistochemical features of RGNT, albeit with focally overlapping DNET-like patterns. Resections of residual or recurrent tumor were performed 1 year and 5 years after the initial resection, but no adjuvant radiation or chemotherapy was given. Ten years after the initial resection, surveillance imaging identified new and enhancing nodules, leading to another gross total resection. This specimen showed areas similar to the original tumor, but also high-grade foci with oligodendroglial morphology, increased cellularity, palisading necrosis, microvascular proliferation, and up to 13 mitotic figures per 10 high power fields. Ancillary studies the status by sequencing showed wild-type of the isocitrate dehydrogenase 1 (IDH1), IDH2, and human histone 3.3 (H3F3A) genes, and *BRAF* studies were negative for mutation or rearrangement. Fluorescence in situ hybridization (FISH) showed codeletion of 1p and 19q

limited to the high-grade regions. By immunohistochemistry there was loss of nuclear alpha-thalassemia mental retardation syndrome, X-linked (*ATR*X) expression only in the high-grade region. Next-generation sequencing showed an fibroblast growth factor receptor receptor 1 (*FGFR*1) kinase domain internal tandem duplication in three resection specimens. *ATR*X mutation in the high-grade tumor was confirmed by sequencing which showed a frameshift mutation (p.R1427fs), while the apparent 1p/19q-codeletion by FISH was due to loss of chromosome arm 1p and only partial loss of 19q. Exceptional features of this case include the temporal lobe location, 1p/19q loss by FISH without true whole-arm codeletion, and anaplastic transformation associated with *ATR*X mutation without radiation or chemotherapy.

Key words: 1p/19q-codeletion, anaplastic transformation, *ATR*X, fibroblast growth factor receptor receptor 1 (*FGFR*1) kinase domain internal tandem duplication, rosette-forming glioneuronal tumor (RGNT).

INTRODUCTION

Rosette-forming glioneuronal tumor (RGNT) is a WHO grade I neoplasm usually occurring adjacent to or within the fourth ventricle, but is also described in other anatomic locations.^{1–4} Histologic findings include two distinct morphologic components, one exhibiting neurocytic rosettes or perivascular pseudorosettes, and another component with fibrillary astrocytic cells similar to pilocytic astrocytoma.⁵ Characteristic molecular alterations include activating mutations in the phosphatidylinositol-4,5-bisphosphate 3-kinase, catalytic subunit alpha gene (*PIK3CA*) structural rearrangements or activating mutations in the fibroblast

Correspondence: Aaron Halfpenny, DO, Oregon Health & Science University, 3181 SW Sam Jackson Park Road, Mail Code L113, Portland, OR 97239, USA. Email: halfpenn@ohsu.edu

Received 22 April 2019; Revised 03 June 2019; Accepted 24 June 2019; published online 21 August 2019.

© 2019 The Authors. *Neuropathology* published by John Wiley & Sons Australia, Ltd on behalf of Japanese Society of Neuropathology

This is an open access article under the terms of the Creative Commons Attribution-NonCommercial-NoDerivs License, which permits use and distribution in any medium, provided the original work is properly cited, the use is non-commercial and no modifications or adaptations are made.

growth factor receptor 1 gene (*FGFR1*), although these are not specific to RGNT.⁶ Some examples show morphologic and genetic overlap with dysembryoplastic neuroepithelial tumor (DNET), and this differential diagnosis can be challenging.⁷ RGNTs are rarely reported to undergo anaplastic change, with most examples occurring in association with radiation treatment.^{2,3} In the central nervous system, alpha-thalassemia with mental retardation syndrome, X-linked gene (*ATRX*) mutations are typically associated with infiltrating astrocytomas with *IDH* gene mutations, and are also frequently seen in high-grade gliomas with histone H3 p.K27M and H3.3 p.G34R or p.G34V mutations.⁸ More recently, *ATRX* mutations have been associated with high-grade transformation in tumors histologically categorized as pilocytic astrocytomas.⁹ Here, we report a case of a recurrent epilepsy-associated tumor histologically compatible with RGNT that showed anaplastic transformation and acquisition of an *ATRX* mutation in the absence of radiation or chemotherapy.

CLINICAL SUMMARY AND PATHOLOGIC FINDINGS

A 1-year-old girl presented with developmental delay and seizures. Magnetic resonance imaging (MRI) identified a cystic temporal lesion (Fig. 1A). She was monitored by imaging until age 5, when new enhancement and growth of the lesion prompted a near total surgical resection. Histopathological findings were observed on the resected tissuesections stained with hematoxylin and eosin (HE). This specimen showed a moderately cellular neoplasm of monomorphic cells with round nuclei, perinuclear halos, a mucin-rich background, and neurocytic rosettes (Fig. 1B). Other areas showed piloid cells with long thin processes and spindled nuclei (Fig. 1C). Synaptophysin immunoreactivity was intense and highlighted neuropil cores within the rosettes (Fig. 1D). Floating neurons and nodular architecture were not identified. The pathologic diagnosis at the initial resection was extraventricular neurocytoma with a focal DNET-like pattern, WHO grade II.

This patient subsequently underwent surgical gross total resection (GTR) of residual tumor at age 6, prompted by worsening epilepsy, and another GTR at age 11 for recurrent tumor. These resections were diagnosed as residual/recurrent extraventricular neurocytoma. Surveillance MRI at age 15 showed new nodular enhancement in the resection cavity (Fig. 1E), prompting a third GTR for recurrent disease. This most recent specimen showed regions resembling the original tumor (Fig. 1F). However, other areas showed high-grade features with histology that closely resembled anaplastic oligodendroglioma (Fig. 1G). This included hypercellular sheets of cells with rounded

nuclei and perinuclear cytoplasmic clearing, microvascular proliferation, palisading necrosis, and up to 13 mitotic figures per 10 high power fields. *ATRX* immunohistochemistry showed loss of nuclear staining in the high-grade regions of tumor (Fig. 1H), and *ATRX* expression was retained in the low-grade portion. Additional immunohistochemistry showed scattered neurofilament-positive processes, scattered neuronal nuclear antigen-positive cells, and CD34 staining of vascular endothelial cells only. The Ki-67 labeling index was less than 2% in low-grade areas, and up to 20% in high-grade areas. Oligodendrocyte transcription factor 2 (*OLIG2*) was strongly positive in the tumor cells in both areas. This feature argued against a neurocytic neoplasm, and taken with the unusual clinical history and high-grade histology, prompted additional molecular studies and reconsideration of the initial diagnosis.

Ancillary studies included fluorescence in situ hybridization (FISH) for 1p/19q, which showed codeletion limited to the high-grade areas (Fig. 1I). Sanger sequencing of the genes for isocitrate dehydrogenase 1 (*IDH1*), *IDH2*, human histone 3.3 (*H3F3A*) was negative for mutations. No *BRAF* fusions were detected by FISH. To clarify the diagnosis and the relationship between the high-grade specimen and the previous low-grade neoplasm, next-generation sequencing (NGS) studies were performed on tumor samples from the initial resection, the second recurrence, and the third recurrence which included the high-grade histology. The UCSF 500 Cancer Gene Panel is a hybrid capture-based NGS platform assessing mutation status of over 500 cancer-associated genes, common gene fusions, and whole-genome copy number profiling.¹⁰ This analysis showed an *FGFR1* kinase domain internal tandem duplication, with identical duplication breakpoints seen in all three specimens (Fig. 1J, 5' duplication boundary within exon 10 and 3' duplication boundary within introns 18-19). This alteration is predicted to result in an in-frame tandem duplication of *FGFR1* codons 438-795, containing the intracellular tyrosine kinase domain.¹¹ Sequencing also identified a p.R1427fs truncating *ATRX* mutation only in the third recurrence specimen, with a mutant allele frequency of 22%. The *ATRX* mutant allele was not detected in the previous specimens, with 408 reads at this locus from the initial resection specimen and 503 reads from the second recurrence specimen. Whole-genome copy number profiling of the most recent specimen showed complete loss of chromosome arm 1p, but only partial loss of chromosome arm 19q, not the whole-arm codeletion that is a required component for an integrated diagnosis of oligodendroglioma (Fig. 1K). A few distinct copy number alterations were seen across the three specimens, but the only shared abnormality other than *FGFR1* internal tandem duplication was monosomy 22q. Integrating the

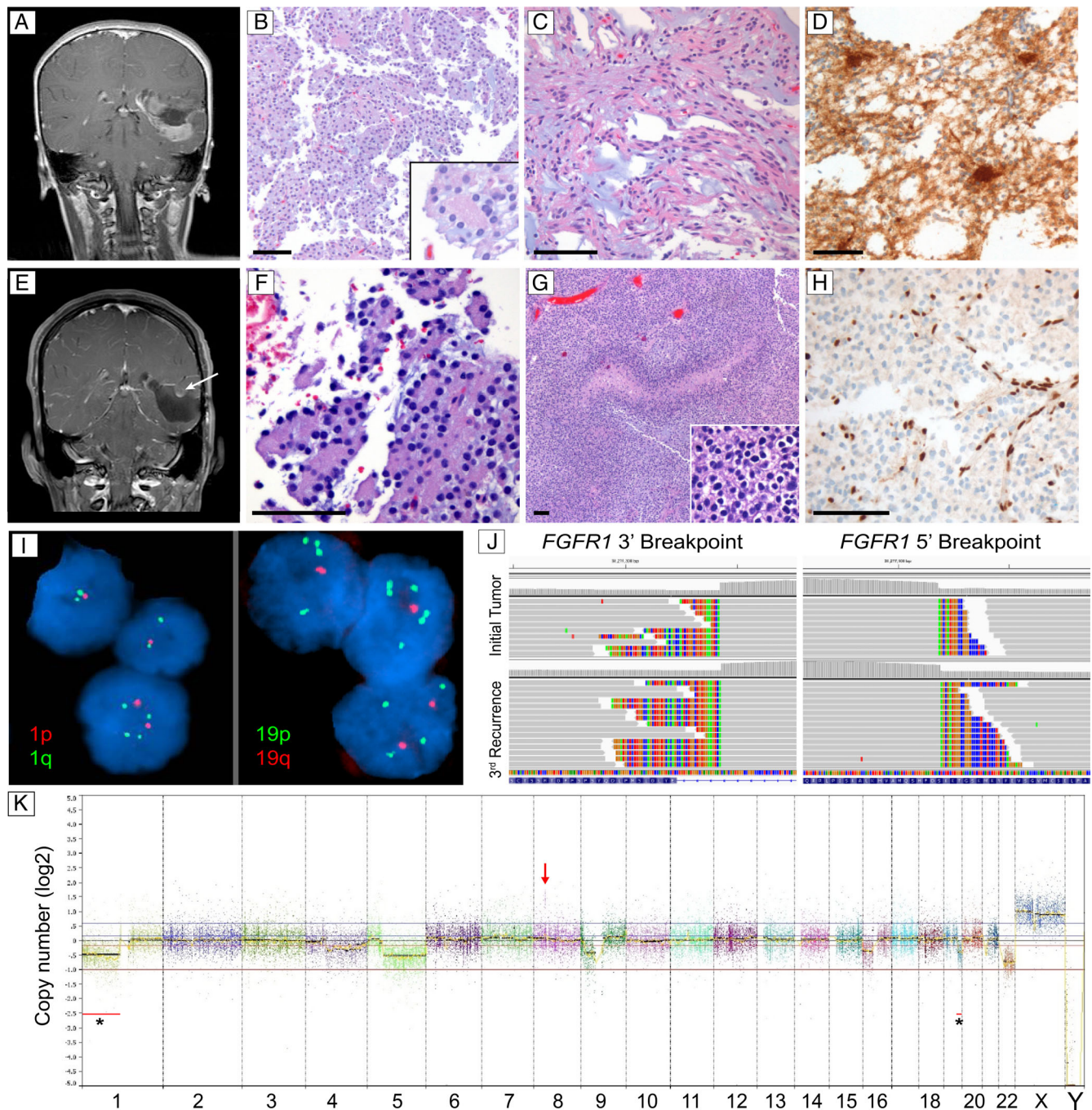


Fig. 1 MRI findings of the brain (A, E), histopathological observations on the tumor sections stained with H&E (B, C, F, G) and immunohistochemical observations (D, H), FISH analysis of the tumor (I), and gene analyses of the tumor (J, K). The tumor is located at the left temporal lobe detected on T1-weighted post-contrast coronal views at 3 years old (A) and 15 years old (E), prior to the most recent GTR. New nodular enhancement appears at the resection cavity (E, arrow). Histological examinations on H&E-stained sections show neurocytic cells, rosettes (B, inset), a mucoid background, and piloid features with elongated nuclei at 3 years old (B, C) and at the initial resection. The most recent GTR tissue shows low-grade and high-grade features (F, G). Synaptophysin immunoreactivity is detected in the initial resection tissue (D), while ATRX immunoreactivity is undetectable in the most recent GTR tissue (H). FISH analysis shows the results consistent with 1p/19q codeletion in the high-grade areas (I). Sequencing traces of the most recent GTR tissue shows 5 duplication boundary within exon 10 and 3 duplication boundary within introns 18-19 (J). Whole-genome copy number profiling on the most recent GTR tissue shows whole-arm 1p loss and only partial loss of chromosome arm 19q (asterisks) and focal copy number gain on chromosome 8 representing *FGFR1* kinase domain tandem duplication (red arrow). Scale bars: 100 μ m (A–H).

molecular and histologic findings across all of these specimens, a revised diagnosis of high-grade neoplasm, most consistent with anaplastic RGNT was rendered. The patient has since completed a course of radiation therapy. She experienced a temporary increase in seizure activity, but is otherwise well, and surveillance imaging has not identified tumor recurrence at approximately 11 months after the most recent resection.

DISCUSSION

The conservation of the *FGFR1* kinase domain internal tandem duplication establishes this patient's case as a single tumor with multiple recurrences over approximately 14 years before undergoing spontaneous (i.e. without radiation therapy) anaplastic progression. After review of multiple specimens and external review, this tumor was determined to be most consistent with RGNT. Other entities were considered in the differential diagnosis, including DNET and extraventricular neurocytoma. The initial diagnosis of extraventricular neurocytoma with a focal DNET-like pattern was excluded largely on the basis of strongly positive OLIG2 immunohistochemistry which was not available at our institution at the time of the initial diagnosis. DNET is a more difficult entity to definitively exclude, given the morphologic overlap with RGNT. However, the findings of distinctly synaptophysin-positive neurocytic rosettes and areas with elongated cells with piloid processes are more typically seen in RGNT than DNET. The lack of conventional DNET cytologic and architectural features in any specimen such as floating neurons, nodularity, and a columnar organization to the glioneuronal element also argue against DNET and favor RGNT. While criteria for anaplastic RGNT are not defined, the presence of numerous mitotic figures, necrosis, and microvascular proliferation support the designation of anaplastic change in this particular case.

Targeted NGS has been shown to be of great benefit in the pediatric neuro-oncology population, and in this case NGS results helped to arrive at a more precise diagnosis and provided an explanation for the unusual constellation of *ATRX* loss, wild-type *IDH1* and *IDH2*, and apparent 1p/19q-codeletion by FISH. The 1p/19q-codeletion in this setting introduced pediatric-type oligodendroglioma into the differential diagnosis, although this codeletion is seen in only a minority of pediatric-type oligodendrogliomas and they are predominantly low grade.¹² Subsequent identification of only partial loss of 19q by whole-genome copy number profiling illustrates that methodologies for detection of whole-arm 1p and 19q loss should be considered as an adjunct to 1p/19q codeletion by FISH when apparent codeletion is unaccompanied by *IDH* mutation. The finding of *ATRX*

immunohistochemistry loss limited to high-grade regions of this tumor, accompanied by a confirmed *ATRX* mutation, suggests that RGNT may be another tumor in which *ATRX* gene mutation could be a potential driver of anaplastic progression. Finally, this case shows that the diagnosis of RGNT should not necessarily be restricted by anatomic location despite a preponderance of cases occurring near the fourth ventricle. A tumor with distinct neurocytic and piloid components and appropriate mutations such as *PIK3CA* or *FGFR1* should prompt consideration of the diagnosis regardless of location. While the behavior of RGNTs is thought to be relatively indolent, anaplastic progression can occur even in the absence of radiation therapy.

ACKNOWLEDGMENTS

The authors are thankful to the patient and their family for allowing us to share this case.

DISCLOSURE

The authors declare they have no competing interests.

REFERENCES

- Allinson KS, O'Donovan DG, Jena R, Cross JJ, Santarius TS. Rosette-forming glioneuronal tumor with dissemination throughout the ventricular system: A case report. *Clin Neuropathol* 2015; **34**: 64–69.
- Garcia Cabezas S, Serran Blanch R, Sanchez-Sanchez R, Palacios Eito A. Rosette-forming glioneuronal tumour (RGNT) of the fourth ventricle: A highly aggressive case. *Brain Tumor Pathol* 2014; **32**: 124–130.
- Scholz M, Hoischen A, Radlwimmer B *et al.* Rosetted glioneuronal tumor of the spine with overtly anaplastic histologic features. *Acta Neuropathol* 2009; **117**: 591–593.
- Yang C, Fang J, Li G *et al.* Histopathological, molecular, clinical and radiological characterization of rosette-forming glioneuronal tumor in the central nervous system. *Oncotarget* 2017; **8**: 109175–109190.
- Hainfellner JA, Giangaspero F, Rosenblum MK, Gessi M, Preusser M. Rosette-forming glioneuronal tumor. In: Louis DN, Ohgaki H, Wiestler OD, Cavenee WK, (eds). *WHO Classification of Tumors of the Central Nervous System*, 4th edn. Lyon: International Agency for Research on Cancer, 2016; 150–151.
- Gessi M, Moneim YA, Hammes J *et al.* FGFR1 mutations in rosette-forming glioneuronal tumors of the fourth ventricle. *J Neuropathol Exp Neurol* 2014; **73**: 580–584.
- Komori T, Scheithauer BW, Hirose T. A rosette forming glioneuronal tumor of the fourth ventricle: Infratentorial form of dysembryoplastic neuroepithelial tumor? *Am J Surg Pathol* 2002; **26**: 582–591.

8. Appin CL, Brat DJ. Molecular genetics of gliomas. *Cancer J* 2014; **20**: 66–72.
9. Reinhardt A, Stichel D, Schrimpf D *et al.* Anaplastic astrocytoma with piloid features, a novel molecular class of IDH wildtype glioma with recurrent MAPK pathway, CDKN2A/B and ATRX alterations. *Acta Neuropathol* 2018; **136**: 273–291.
10. Kline CN, Joseph NM, Grenert JP *et al.* Targeted next-generation sequencing of pediatric neuro-oncology patients improves diagnosis, identifies pathogenic germline mutations, and directs targeted therapy. *Neuro Oncol* 2016; **19**: 699–709.
11. Zhang J, Wu G, Miller CP *et al.* Whole-genome sequencing identifies genetic alterations in pediatric low-grade gliomas. *Nat Genet* 2013; **6**: 602–612.
12. Rodriguez F, Tihan T, Lin D *et al.* Clinicopathologic features of pediatric oligodendrogliomas: A series of 50 patients. *Am J Surg Pathol* 2014; **38**: 1058–1070.